Catalytically Inactive Condensation Domain C1 Is Responsible for the Dimerization of the VibF Subunit of Vibriobactin Synthetase†

Nathan J. Hillson, Carl J. Balibar, and Christopher T. Walsh*

Department of Biological Chemistry and Molecular Pharmacology, Harvard Medical School, Boston, Massachusetts 02115

Received May 26, 2004; Revised Manuscript Received June 28, 2004

ABSTRACT: Nonribosomal peptide synthetases (NRPS), fatty acid synthases (FAS), and polyketide synthases (PKS) are multimodular enzymatic assembly lines utilized in natural product biosynthesis. The oligomeric structure of these assembly line enzymes has been a topic of interest because higher order oligomeric quaternary structural arrangements allow for alternate paths of acyl intermediate elongation and present unique challenges for the chimeric engineering of hybrid assembly lines. Unlike other NRPS systems that in general appear to be monomeric, the six domain (Cy1-Cy2-A-C1-PCP-C2) VibF subunit of vibriobactin synthetase has previously been shown to be dimeric, the same oligomeric state as that observed for FAS and PKS assembly lines. It has been demonstrated that the C1 domain within VibF is catalytically inactive and is not required for vibriobactin production. Utilizing sedimentation equilibrium analytical ultracentrifugation experiments to determine the oligomeric states of several VibF subfragments, we report that the C1 domain is largely responsible for VibF dimerization. Comparative rates of vibriobactin production, coupled with dissociation constants for VibF subfragment pair heterocomplexes, suggest that the mere presence of C1 does not detectably enhance the catalytic rates of neighboring domains, but it may properly orient Cy1-Cy2-A relative to PCP-C2.

Nonribosomal peptide (NRP),[1] fatty acid (FA), and polyketide (PK) natural products are biosynthesized on multimodular enzymatic assembly lines (*1*−*3*). Each module contains catalytic domains for recognition of an amino acid (NRP) or acyl CoA monomer (PK/FA), subsequent covalent loading of the activated monomer in thioester linkage onto the pantetheinyl prosthetic arm of the carrier protein domain, and bond formation as the acyl-*S*-enzyme intermediates are sequentially transferred to downsteam modules in an elongating cascade through the carrier protein domain pantetheinyl tethers. The nature of the oligomeric structure of these assembly line enzymes has been a topic of interest because higher order oligomeric quaternary structural arrangements allow for alternate paths of elongation, because the cascade of intermediates could flow to carrier protein domains on the same (intrachain) or neighboring (interchain) assembly lines. For the dimeric deoxyerythronolide B polyketide synthase (PKS) and animal fatty acid synthase (FAS) systems, it has been shown that indeed both intra- and interchain elongation cycles transpire (*4*, *5*). In contrast, it appears that NRP assembly lines generally operate in a monomeric fashion (*6*), heavily constraining interchain processing.

Currently, the only example of a NRPS system with a higher order oligomeric structure is the dimeric VibF subunit of vibriobactin synthetase (*7*−*10*). The vibriobactin synthetase contains three other proteins, VibB, VibE, and VibH, that when purified and mixed with VibF and the substrates ATP, threonine, 2,3-dihydroxybenzoate (DHB), and norspermidine produce the iron chelator vibriobactin (**2**). Production of the siderophore enhances the virulence of *Vibrio cholerae*, the causative agent of cholera, in vertebrate infections (*11*, *12*). Given the ability to reconstitute the full 10 domain assembly line and detect several intermediates, we have previously assigned functions to the six domains of VibF (Cy1-Cy2-A-C1-PCP-C2) (*7*). Heterodimeric mutant complementation experiments establish that the Cy1, Cy2, and A catalytic domains within VibF act on acyl intermediates in both intra- and interchain fashion, while C2 appears to operate predominantly in an intrachain manner (*10*).

The catalytic activities of Cy1-Cy2-A and PCP-C2 have been shown to be sufficient to replace full length VibF in the production of vibriobactin (and thereby leave C1 without a catalytic role) (*7*), as shown in Scheme 1. Although there are other NRPS systems containing subunits with putatively catalytically inactive condensation domains, including AngR in the anguibactin system (*13*) and NRPS-3 in the bleomycin system (*14*), NRPS assembly lines in general rarely contain inoperable domains. This is in direct contrast with PKS systems that often residually house modifying domains harboring mutations at crucial residues that abrogate their

† This work has been supported by the National Institutes of Health (Grant AI42738 to C.T.W.). N.J.H. is a National Science Foundation Graduate Research Fellow. C.J.B. is funded by a Pharmacological Sciences Training Grant through the National Institute of General Medical Sciences.

* To whom correspondence should be addressed. Phone: 617-432-1715. Fax: 617-432-0438. E-mail: christopher_walsh@hms.harvard.edu.

[1] Abbreviations: A, adenylation domain; ArCP, aryl carrier protein; C, condensation domain; Cy, heterocyclization domain; DHB, 2,3-dihydroxybenzoate; DHP, 2,3-dihydroxyphenyl; DTT, dithiothreitol; E, epimerization domain; FA, fatty acid; FAS, fatty acid synthase; ICL, isochorismate lyase; mOx, 5-methyloxazoline; MT, methyl transferase domain; NRP, nonribosomal peptide; NRPS, nonribosomal peptide synthetase; Ox, oxidation domain; PCP, peptidyl carrier protein; PK, polyketide; PKS, polyketide synthase; TCEP, tris(carboxyethyl)phosphine.

10.1021/bi0489199 CCC: $27.50
Published on Web 08/06/2004

Scheme 1

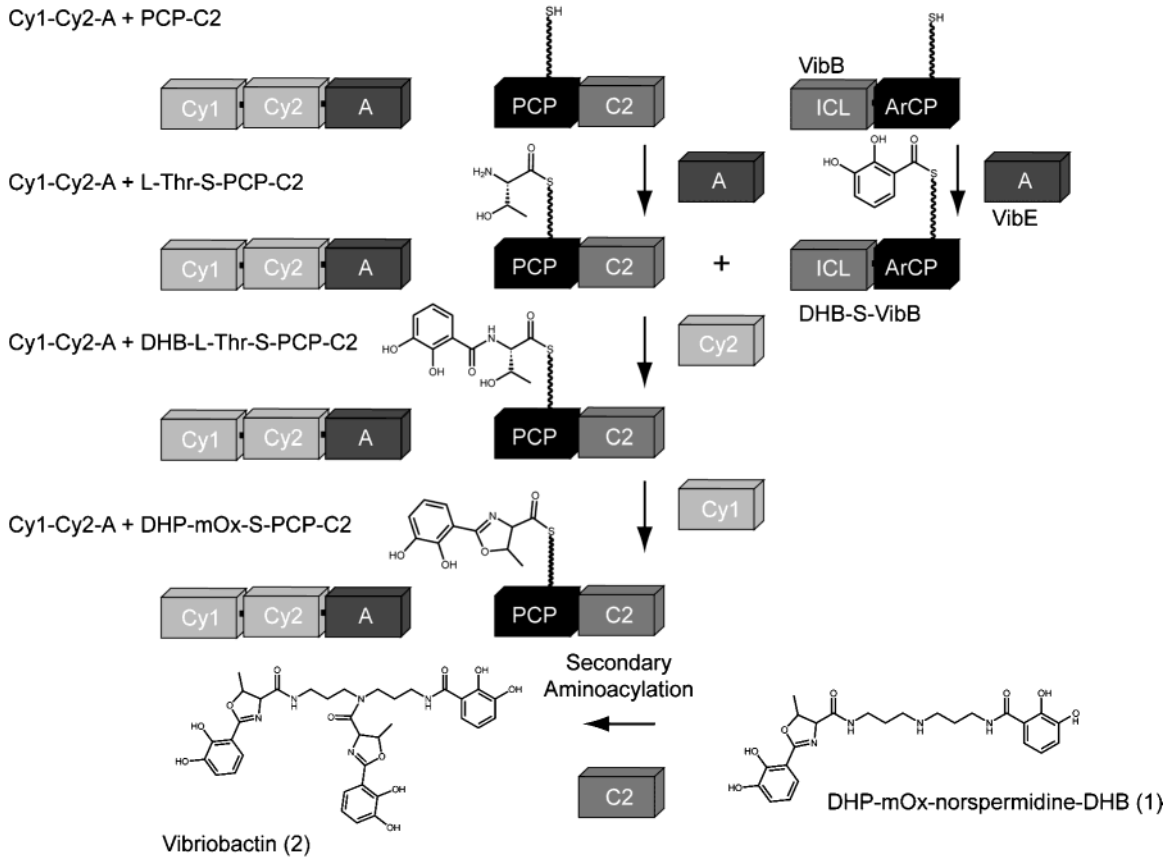

function (*15*−*17*). C1 is additionally set apart from other condensation domains in that its location in VibF (Cy1-Cy2-A-**C1**-PCP-C2) differs from that found in the canonical NRPS repeat (-**C**-A-PCP-), and C1 resides in a location normally reserved for modifying (e.g., MT, Ox, and E) domains (*3*, *18*, *19*). Since no catalytic task is asked of C1, it presumably could play a supportive structural role. C1 may be responsible for the dimerization of VibF, or its presence may promote productive conformations of neighboring catalytic domains. This study investigates these two prospects for C1, namely, interrogating the influence of C1 on the oligomeric state of VibF and comparing vibriobactin production rates in the absence or presence of C1.

EXPERIMENTAL PROCEDURES

Materials and General Methods. 2,3-DHB, coenzyme A, and L-threonine were purchased from Sigma-Aldrich Chemical Co. ATP was purchased from Boehringer Mannheim. TCEP was purchased from Fluka. DHP-mOx-norspermidine-DHB (**1**) was obtained as described previously (*9*). Standard recombinant DNA techniques and microbiological procedures were performed as described (*20*). Restriction enzymes and T4 DNA ligase were purchased from New England Biolabs. *Pfu* polymerase was purchased from Stratagene. Competent *Escherichia coli* were purchased from Invitrogen. Oligonucleotide primers were purchased from Integrated DNA Technologies, and DNA sequencing to verify the fidelity of amplification was performed on double-stranded DNA by the Molecular Biology Core Facilities of the Dana Farber Cancer Institute (Boston, MA). Ni-NTA Superflow resin was purchased from Qiagen.

Design, Expression, and Purification of VibF Subfragments. Expression plasmids for two subfragments, Cy1-Cy2-A (pETCyCyA) and PCP-C2 (pETPCPC2), had been constructed previously (*9*). DNA encoding C1 was amplified from pVibF (*8*) by use of the following primers: C1nf, 5′-CTCTGTTCATATGGTAGGTCAAGCGAATCAAAGTC-3′; C1nr, 5′-GTTCATCACGTACGAAATTGAGTC-3′; C1cf, 5′-GTCACTGCCGGATATCGAAAAGCAGCTGCAAAC-3′; C1cr, 5′-GCACTCGAGAACCGCAGAGGAATTTA-CAGCGCTCAATTC-3′ (restriction sites underlined). The Cy1-Cy2-A-C1 expression plasmid (pETCyCyAC1) was made by amplifying with C1cf and C1cr, digesting with *Eco*RV and *Xho*I and ligating into similarly digested pET-CyCyA. The C1 expression plasmid (pETC1) was made by amplifying with C1nf and C1cr, digesting with *Nde*I and *Xho*I and ligating into similarly digested pETCyCyA. The C1-PCP-C2 expression plasmid (pETC1PCPC2) was made by amplifying with C1nf and C1nr, digesting with *Nde*I and *Bsi*WI, and ligating into similarly digested pETPCPC2. Expression plasmids were transformed into competent *E. coli* BL21(DE3). All subfragments used in this study are shown (along with wild-type VibF for comparison) in Scheme 2 and were expressed and purified identically to the method previously reported for Cy1-Cy2-A and PCP-C2 (*9*).

Analytical Ultracentrifugation. Sedimentation equilibrium experiments were performed with a Beckman Optima XL-A. Equilibrium and Monte Carlo analyses were conducted with UltraScan, version 6.0 (*21*). Hydrodynamic corrections for buffer conditions were made according to data published by Laue et al. (*22*), and the partial specific volume of the VibF subfragments was estimated according to the method

Scheme 2

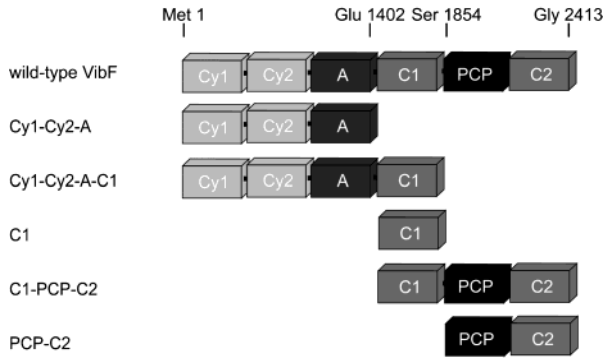

of Cohn and Edsall (*23*), as implemented in UltraScan. VibF subfragment samples were analyzed in buffer containing 20 mM Tris, pH 8, 50 mM NaCl, 2 mM $MgCl_2$, 1 mM dithiothreitol (DTT), and 10% glycerol at 4 °C at speeds ranging between 6600 and 32 000 rpm. Samples were spun in a 6-channel 12 mm external fill equilibrium centerpiece in an An-60 Ti rotor. Scans (280 nm) were collected at equilibrium in radial step mode with 0.001 cm steps and 20 point averaging. Loading concentrations were 0.70, 0.40, and 0.20 OD, and data exceeding 0.9 OD were excluded. The molar extinction coefficients for the VibF subfragments (in M^{-1} cm^{-1} at 280 nm) are as follows: Cy1-Cy2-A, 169 580; Cy1-Cy2-A-C1, 221 650; C1, 52 070; C1-PCP-C2, 124 810; PCP-C2, 72 740. Data fitting was performed with one-component or monomer−dimer equilibrium models (individual subfragments), and two-component or heteroassociation models (subfragment pairs at a 1:1 stoichiometry) as implemented in UltraScan with the exception of the C1 subfragment, which was fitted with a monomer−dimer−tetramer model.

Assay of VibF Subfragment Pairs. Vibriobactin formation was assayed identically to that previously reported for Cy1-Cy2-A and PCP-C2 (*7*) with 4 μM N-terminal subfragment (Cy1-Cy2-A or Cy1-Cy2-A-C1) and 10 μM C-terminal subfragment (C1-PCP-C2 or PCP-C2). A representative assay, that for the Cy1-Cy2-A and PCP-C2 pair, is shown in Scheme 1.

RESULTS

VibF Subfragment Design and Construction. Expression plasmids for Cy1-Cy2-A and PCP-C2 had been constructed previously (*9*). In VibF residue numbering, Cy1-Cy2-A extends from M1 to E1402 and PCP-C2 extends from S1854 to G2413, operationally defining the C1 domain from P1403 to L1853 (Scheme 2). With this definition of the C1 domain and consideration of molecular biology constraints, we designed three new VibF subfragments: Cy1-Cy2-A-C1 (M1 to V1861), C1-PCP-C2 (V1404 to G2413), and a stand alone C1 (V1404 to V1861). These three constructs were created by standard PCR and molecular biology techniques using the primers and vectors described in Experimental Procedures. The three constructs were verified by DNA sequencing.

Purification of VibF Subfragments. Expression and purification of Cy1-Cy2-A-C1, C1-PCP-C2, and C1 were identical to that previously reported for Cy1-Cy2-A and PCP-C2 (*7*). Briefly, all constructs were expressed in *E. coli* as

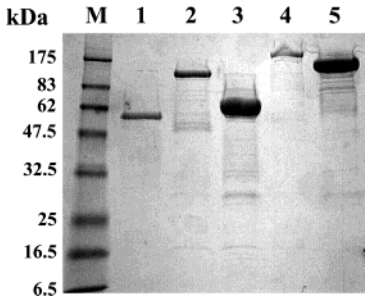

FIGURE 1: SDS-12% PAGE of the VibF subfragment constructs: M, molecular weight standards; lane 1, C1 51.6 kDa; lane 2, C1-PCP-C2 114.0 kDa; lane 3, PCP-C2 62.3 kDa; lane 4, Cy1-Cy2-A-C1 208.5 kDa; lane 5, Cy1-Cy2-A 158.0 kDa.

C-terminal His-tag fusion proteins and purified by nickel affinity chromatography. All proteins were obtained in comparable yield and purity, and migration on SDS-12% PAGE of the constructs was consistent with the calculated masses of Cy1-Cy2-A 158.0 kDa, Cy1-Cy2-A-C1 208.5 kDa, C1 51.6 kDa, C1-PCP-C2 114.0 kDa, and PCP-C2 62.3 kDa (Figure 1).

Sedimentation Equilibrium Analytical Ultracentrifugation of VibF Subfragments and Subfragment Mixture Complexes. Analytical ultracentrifugation was utilized as a physical measurement to determine the oligomeric states of the VibF subfragments and identify putative stable complexes formed within mixtures of multiple subfragments. For the global equilibrium analysis of the subfragments, scans at various speeds and loading concentrations (see Experimental Procedures) of each subfragment were well fit with monomer−dimer equilibrium models (with the exception of PCP-C2 scans, which were sufficiently described with a monomer-only model, and C1 scans, which were well explained with a monomer−dimer−tetramer model), resulting in random residuals (Table 1, first row for each subfragment). Representative scans and residuals for Cy1-Cy2-A-C1 and PCP-C2 are shown in Figure 2A−D. Those for Cy1-Cy2-A, C1, and C1-PCP-C2 are not shown, but their respective fit variances (error metric) and percentage number of runs observed (residual randomness metric) are sufficient to indicate comparable fits to those shown in Figure 2. (Generally speaking, it is desirable to have a fit variance less than 1×10^{-4} and a percentage of number of runs greater than 35% (*21*)). The fitted subfragment molecular masses are consistent with those derived from their respective protein sequences, and the dissociation constants indicate the extent to which each construct is dimeric (or dimeric/tetrameric for C1). It should be noted that the multidomain subfragments containing the C1 domain (Cy1-Cy2-A-C1 and C1-PCP-C2) are observed to be predominantly dimeric, while those lacking it (Cy1-Cy2-A and PCP-C2) are mostly monomeric at the experimental conditions. The stand-alone C1 subfragment appears to be predominantly dimeric/tetrameric at the experimental conditions.

For comparison with the subfragment equilibrium models presented above, fit variances and percentage number of runs are presented for alternative models of the subfragments (Table 1, rows below the first for each subfragment). For PCP-C2, the monomer-only model performs indistinguishably from the monomer−dimer equilibrium model, indicating that there is no detectable dimeric PCP-C2 at the experimental concentrations. For Cy1-Cy2-A, the monomer−dimer

Table 1: Oligomeric Models for VibF Subfragments

subfragment	model	variance (10^{-4})	no. runs (%)	fitted mass (kDa)	exp. mass (kDa)	fitted K_d
Cy1-Cy2-A	monomer−dimer equil	0.628 ± 0.030	41.4	157.6 ± 4.5	158.0	27.3 ± 8.5 μM
	monomer	0.860 ± 0.041	34.4	158.0 ± 0.9	158.0	*a*
	dimer	7.75 ± 0.44	16.1	316.3 ± 7.0	316.1	*a*
Cy1-Cy2-A−C1	monomer−dimer equil	0.743 ± 0.040	36.3	209.2 ± 9.5	208.5	118 ± 64 nM
	dimer	0.870 ± 0.043	34.9	416.9 ± 3.1	417.0	*a*
	monomer	1.62 ± 0.10	24.4	209.1 ± 5.5	208.5	*a*
C1	monomer−dimer−tetramer equil	0.311 ± 0.030	36.8	51.8 ± 1.4	51.6	176 ± 51 nM; 0.410 ± 0.394 μM^3
	dimer−tetramer equil	0.323 ± 0.032	33.8	103.0 ± 3.0	103.2	1.50 ± 0.46 μM
	monomer−tetramer equil	0.412 ± 0.038	29.6	51.7 ± 0.6	51.6	4.70 ± 0.58 μM^3
	monomer−dimer equil	7.69 ± 0.64	7.60	52.2 ± 2.0	51.6	0.273 ± 0.263 nM
C1−PCP−C2	monomer−dimer equil	0.731 ± 0.053	39.0	114.6 ± 5.6	114.0	366 ± 204 nM
	dimer	0.897 ± 0.053	34.8	227.9 ± 2.6	228.0	*a*
	monomer	2.86 ± 0.24	20.1	114.1 ± 4.8	114.0	*a*
PCP−C2	monomer	0.816 ± 0.046	42.1	62.3 ± 0.4	62.3	*a*
	monomer−dimer equil	0.813 ± 0.048	42.3	61.9 ± 0.6	62.3	2.43 ± 1.88 mM
	dimer	14.1 ± 1.0	14.4	125.4 ± 3.7	124.6	*a*

[a] Not applicable.

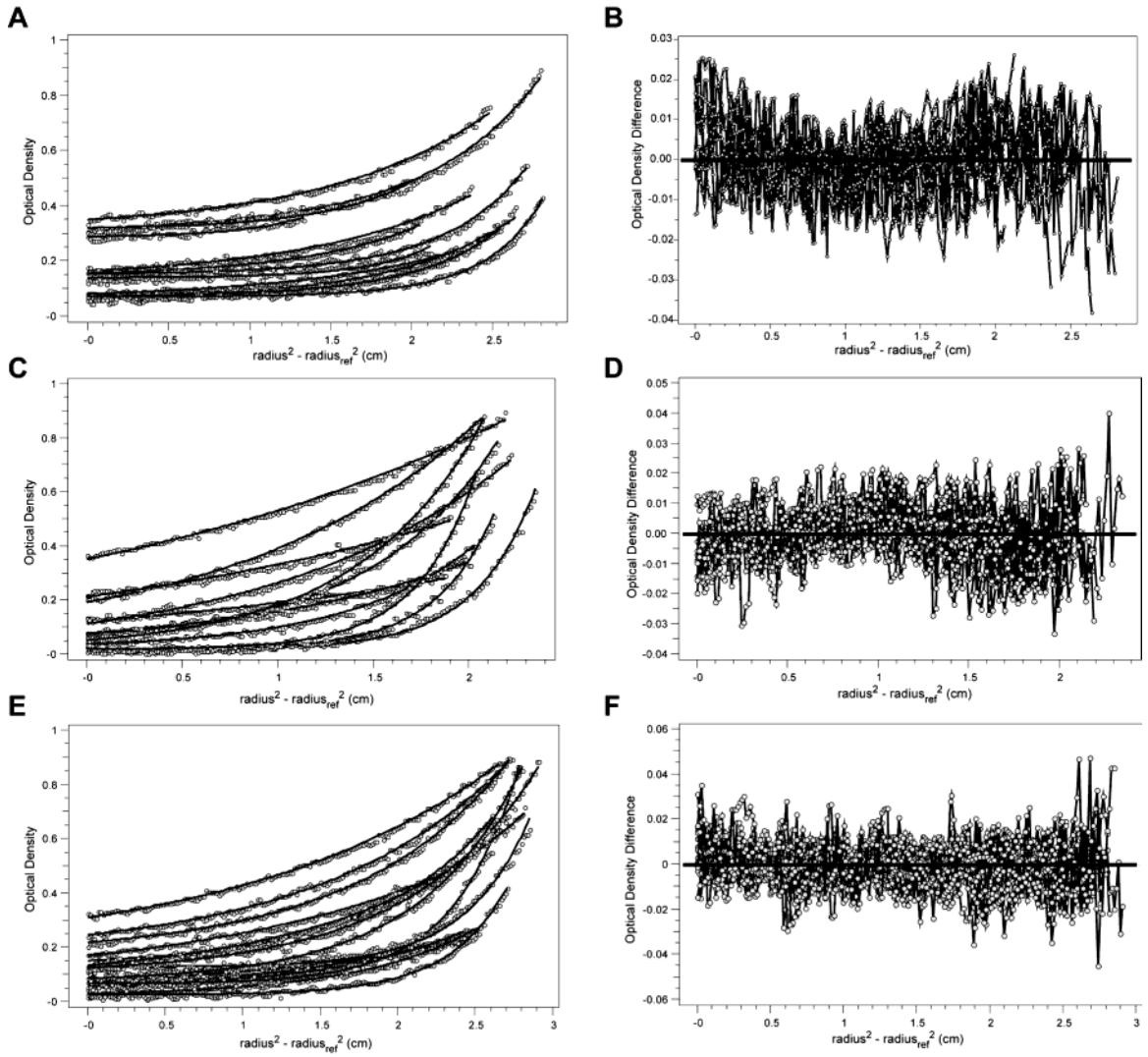

FIGURE 2: Sedimentation equilibrium analytical ultracentrifugation analysis of representative VibF subfragments and subfragment pairs: (A,B) Cy1-Cy2-A-C1; (C,D) PCP-C2; (E,F) Cy1-Cy2-A + C1-PCP-C2; (A,C,E) overlays of wavelength scans; (B,D,F) residuals from the global fits of the data as described under Experimental Procedures.

equilibrium model fit has a statistically significant ($P < 0.001$) lower variance than the monomer-only model, but the latter's variance and percentage number of runs is still quite reasonable. On the other hand, the Cy1-Cy2-A dimer-only model has a fit variance that is an order of magnitude greater than that of the monomer−dimer equilibrium model,

Table 2: Oligomeric Models for VibF Subfragment Pairs

subfragment pair	model	variance (10^{-4})	no. runs (%)	fitted mass 1 (kDa)	fitted mass 2 (kDa)	fitted K_D (μM)
Cy1-Cy2-A + PCP-C2	heteroassoc	0.191 ± 0.031	35.5	64.9 ± 5.3	159.1 ± 11.9	2.17 ± 1.37
	2-component	0.493 ± 0.033	23.7	64.5 ± 14.7	158.0 ± 1.3	*a*
(Cy1-Cy2-A-C1)$_2$ + PCP-C2	2-component	1.47 ± 0.15	44.2	64.4 ± 4.9	415.6 ± 32.1	*a*
	heteroassoc	1.64 ± 0.26	43.6	62.5 ± 4.6	401.0 ± 22.0	1.40 ± 0.92
Cy1-Cy2-A + (C1-PCP-C2)$_2$	2-component	0.845 ± 0.074	43.3	158.3 ± 11.3	228.6 ± 15.5	*a*
	heteroassoc	0.840 ± 0.069	43.7	158.1 ± 10.7	225.7 ± 16.2	6.14 ± 3.41

[a] Not applicable.

and its percentage number of runs suggests systematic residuals (indicative of poor modeling of the experimental data). One caveat to the model comparison is that the monomer−dimer model contains an additional parameter (namely, the dissociation constant), and thus the reduction in fit variance could be less meaningful than it might otherwise appear. The results of the Cy1-Cy2-A model comparisons show that a small amount of dimer is detected with confidence, but that the monomer-only model of Cy1-Cy2-A also performs well. Analogous observations can be made for the other multidomain VibF subfragments fit with monomer−dimer equilibrium models above. The Cy1-Cy2-A-C1 and C1-PCP-C2 dimer-only models are acceptable, but the monomeric forms of these subfragments are detected. For the stand-alone C1 subfragment, the monomer−dimer−tetramer and dimer−tetramer models perform indistinguishably ($P < 0.39$) with similar variances and percentage number of runs. This implies that the monomeric state of C1 is not detectable with confidence. On the other hand, the monomer−dimer−tetramer model has a significantly lower variance than those for the monomer−tetramer and monomer−dimer models ($P < 0.02$ and 0.001, respectively), suggesting that both dimeric and tetrameric states of C1 are observed at the experimental conditions.

One-to-one stoichiometric mixtures of three different subfragment pairs (Cy1-Cy2-A + PCP-C2, Cy1-Cy2-A-C1 + PCP-C2, and Cy1-Cy2-A + C1-PCP-C2) were made to test for the existence of stable subfragment heterocomplexes. Each pair contained an N-terminal (e.g., Cy1-Cy2-A) and a C-terminal (e.g., PCP-C2) VibF subfragment, in the hopes of forming pseudo-monomeric, or dimeric VibF species, or both (e.g., Cy1-Cy2-A·PCP-C2, (Cy1-Cy2-A·PCP-C2)$_2$ or both). For the global equilibrium analysis of the subfragment mixtures, scans at various speeds and loading concentrations (see Experimental Procedures) of each subfragment pair were fit to equilibrium models allocating for complexed and noncomplexed components. Currently, there is only one heteroassociation model available in the UltraScan data fitting package (*21*) (namely, A + B ↔ AB) and there are no options for homoassociation models in the presence of a heterogeneous species, and thus modeling simplifications and approximations were made. As a starting point, noncomplexed Cy1-Cy2-A was approximated by a monomeric-only species, and Cy1-Cy2-A-C1 and C1-PCP-C2 were treated as dimeric-only species. The scans for Cy1-Cy2-A-C1 + PCP-C2 and Cy1-Cy2-A + C1-PCP-C2 could be well described with noninteracting two-component models (i.e., no complex component and one component for each subfragment) and similarly those for Cy1-Cy2-A + PCP-C2 with a heteroassociation model (the two monomeric subfragments complexing into a pseudo-monomeric VibF species (Cy1-Cy2-A·PCP-C2)), resulting in random residuals (Table 2, first row for each subfragment pair). Representative scans and residuals for the Cy1-Cy2-A + C1-PCP-C2 pair are shown in Figure 2E,F. Those for the Cy1-Cy2-A + PCP-C2 and Cy1-Cy2-A-C1 + PCP-C2 pairs are not shown, but their respective fit variances and percentage number of runs observed are sufficient to indicate the quality of their fits. The fitted subfragment molecular masses are consistent with those derived from their respective protein sequences, and the dissociation constant for the Cy1-Cy2-A + PCP-C2 pair indicates the extent to which the pair is modeled to heteroassociate. It should be noted that the sufficiency of noninteracting two-component models for Cy1-Cy2-A-C1 + PCP-C2 and Cy1-Cy2-A + C1-PCP-C2 to yield random residuals (and reasonable fit variances) provides evidence against a predominance of pseudo-VibF complexes (e.g., Cy1-Cy2-A-C1·PCP-C2 and (Cy1-Cy2-A·C1-PCP-C2)$_2$) within these mixtures at the experimental conditions.

For comparison with the subfragment pair mixture models presented above, fit variances and percentage number of runs are also presented for the heteroassociation models for Cy1-Cy2-A-C1 + PCP-C2 and Cy1-Cy2-A + C1-PCP-C2 and for the noninteracting two-component model for Cy1-Cy2-A + PCP-C2 (Table 2, second row for each subfragment pair). For Cy1-Cy2-A-C1 + PCP-C2 and Cy1-Cy2-A + C1-PCP-C2, the fit variance of the heteroassociation model is not significantly smaller ($P < 0.48$) than that of the noninteracting two-component model. Given the experimental concentrations of the subfragments within the mixtures and the best fit dissociation constants, the heteroassociation models suggest substantial conversion of the free subfragments into complexed form. Thus, even though neither of the two model types provides a statistically significant lower variance than the other, their predictions for the extent of complex formation are vastly different. The fitted dissociation constants of the heteroassociation models may be artifactually low, because the heterocomplex species is the highest molecular weight component and as such will be promoted to reduce systematic error resulting from not accounting for all possible species in the subfragment mixture. For the Cy1-Cy2-A + C1-PCP-C2 pair, the presence of the heterocomplex species, namely, Cy1-Cy2-A·(C1-PCP-C2)$_2$, is exploited not only to explain its own contribution to the equilibrium curve but also to implicitly account for the contributions of (Cy1-Cy2-A)$_2$ and (Cy1-Cy2-A·C1-PCP-C2)$_2$, which are not treated explicitly in the simple A + B ↔ AB heteroassociation model. For this reason and because there is no significant difference in the variances of the heteroassociation models and those of the noninteracting two-component models, the fitted dissociation constants should be considered lower limits for Cy1-Cy2-A-C1 + PCP-C2 and Cy1-Cy2-A + C1-PCP-C2. For Cy1-Cy2-A + PCP-C2, the fit variance of the heteroassociation model is significantly smaller ($P <$

0.001) than that of the alternative noninteracting two-component model. Because the noninteracting two-component model is not able to sufficiently explain the observed data, resulting in an unacceptably low percentage of runs observed and a significantly higher variance than the heteroassociation model, we have confidence that we are observing complexation. As was the case above, in the heteroassociation model we have used Cy1-Cy2-A·PCP-C2 to implicitly account for the contributions of $(Cy1\text{-}Cy2\text{-}A)_2$ and $(Cy1\text{-}Cy2\text{-}A{\cdot}PCP\text{-}C2)_2$, and so the dissociation constant for Cy1-Cy2-A + PCP-C2 in Table 2 should somewhat be considered a lower limit. On the other hand, the unaccounted for presence of $(Cy1\text{-}Cy2\text{-}A)_2$ alone cannot fully explain the data, because the monomeric model above in Table 1 for the Cy1-Cy2-A subfragment does not result in excessively nonsystematic residuals and the fitted dissociation constant for the Cy1-Cy2-A homodimerization is an order of magnitude larger than that found for the Cy1-Cy2-A + PCP-C2 heteroassociation model.

Comparative Assay of Vibriobactin Formation Kinetics in the Presence or Absence of the C1 Domain. Beyond its influence on the oligomeric state of VibF, it is possible that C1 structurally perturbs its neighboring catalytic domains, resulting in accelerated vibriobactin production compared with that observed in the absence of C1. To test this, the comparative rates of vibriobactin production were measured for four pairs of VibF subfragments, namely, Cy1-Cy2-A + PCP-C2, Cy1-Cy2-A-C1 + PCP-C2, Cy1-Cy2-A + C1-PCP-C2, and Cy1-Cy2-A-C1 + C1-PCP-C2. Time courses of vibriobactin production from 0 to 10 min for the four pairs is shown in Figure 3A, and the initial linear rates of vibriobactin production (Table 3, second column) were obtained from fitting the time points before the DHP-mOx-norspermidine-DHB (**1**) substrate becomes limiting (Figure 3B). Using the dissociation constants listed in Table 2, and assuming an approximate dissociation constant of 242 ± 108 nM (the mean of those for Cy1-Cy2-A-C1 and C1-PCP-C2 in Table 1) for Cy1-Cy2-A-C1·C1-PCP-C2 (in equilibrium with Cy1-Cy2-A-C1 and C1-PCP-C2 homodimers with roughly equivalent dissociation constants), k_{cat} values (Table 3, last column) for the four heterocomplexes were derived from the initial rates of production. Even with the considerable error bars about the approximate mean dissociation constant for Cy1-Cy2-A-C1·C1-PCP-C2, very small deviations in complex concentration are predicted, reducing concern that its derived k_{cat} value is largely a consequence of the particular dissociation constant chosen. The k_{cat} value for Cy1-Cy2-A-C1·C1-PCP-C2 is larger ($P < 0.001$) than that for the other three pairs, but not alarmingly so. The other three pairs have comparable k_{cat} values with no statistically significant difference between them ($P < 0.20$ or more for all three pairings). Furthermore, the dissociation constants presented in Table 2 are to be considered lower limits for Cy1-Cy2-A + PCP-C2, Cy1-Cy2-A-C1 + PCP-C2 and Cy1-Cy2-A + C1-PCP-C2, and this putatively decreases the expected concentrations of their complexes and thus reduces the respective rate gaps between them and the Cy1-Cy2-A-C1 + C1-PCP-C2 pair.

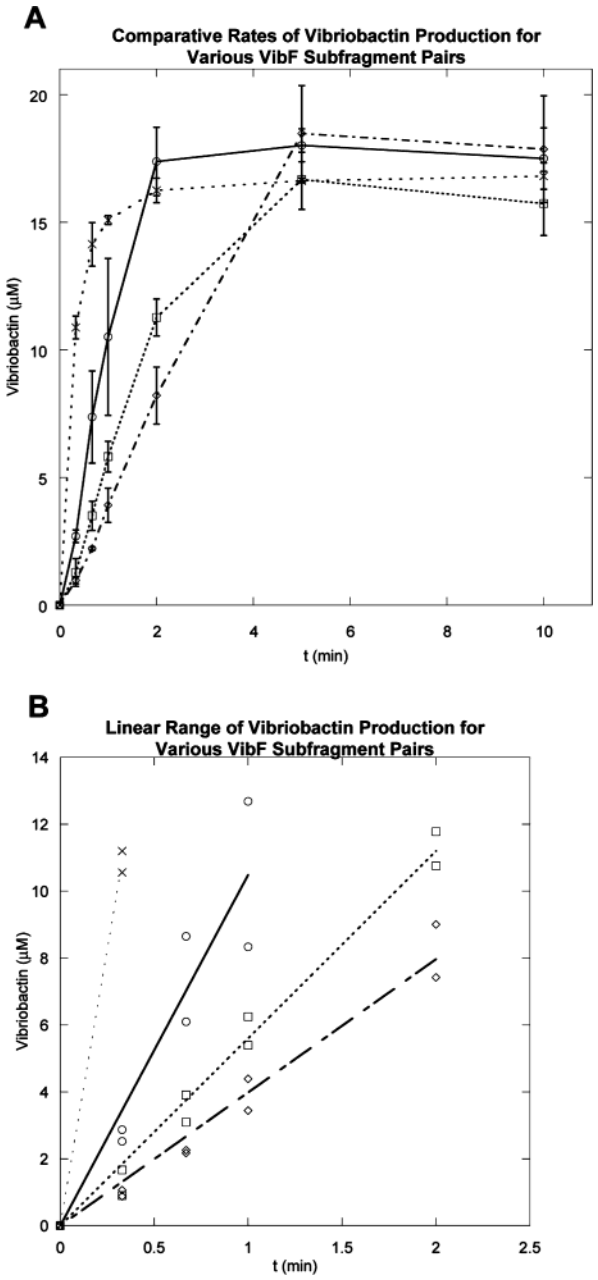

FIGURE 3: Comparative rates of vibriobactin production for VibF subfragment pairs: (A) production of vibriobactin plateaus once the DHP-mOx-norspermidine-DHB substrate becomes limiting; (B) linear range of vibriobactin production at initial time points; (○) Cy1-Cy2-A + PCP-C2; (□) Cy1-Cy2-A-C1 + PCP-C2; (◇) Cy1-Cy2-A + C1-PCP-C2; (×) Cy1-Cy2-A-C1 + C1-PCP-C2.

DISCUSSION

The C1 domain of VibF is unusual in that it does not play a catalytic role and also in that its location differs from that found in the canonical NRPS repeat (*7*). These two observations suggest that C1 may have been evolutionarily inserted between the A and PCP domains of a precursor to VibF or, alternatively, left behind as an evolutionary relic. Assuming that that selection pressure would have resisted its insertion (or promoted its deletion) unless it improved synthetase fitness, C1 should be important to VibF function. Since no catalytic task is asked of the C1 domain, it is implicated only for a structural role. This study probes the oligomeric states of various VibF subfragments and 1:1 mixtures of subfragment pairs, and subsequently compares vibriobactin production rates in the absence or presence of C1.

Sedimentation equilibrium analytical ultracentrifugation experiments for the various VibF subfragments show that the C1 domain is largely responsible for VibF dimerization:

Table 3: Comparative Assay of Vibriobactin Formation Kinetics

subfragment pair	vibriobactin (μM min^{-1})	complex species	[complex] (μM)	k_{cat} (min^{-1})
Cy1-Cy2-A + PCP-C2	11 ± 1	Cy1-Cy2-A·PCP-C2	3.1 ± 0.4	3.4 ± 0.6
Cy1-Cy2-A-C1 + PCP-C2	5.6 ± 0.2	(Cy1-Cy2-A-C1)$_2$·PCP-C2	1.7 ± 0.1	3.3 ± 0.3
Cy1-Cy2-A + C1-PCP-C2	4.0 ± 0.2	Cy1-Cy2-A·(C1-PCP-C2)$_2$	1.5 ± 0.3	2.7 ± 0.6
Cy1-Cy2-A-C1 + C1-PCP-C2	33 ± 1	Cy1-Cy2-A-C1·C1-PCP-C2	2.6 ± 0.1	12 ± 1
wild-type VibF (*10*)	*a*	Cy1-Cy2-A-C1-PCP-C2	*a*	48

[a] Not applicable.

PCP-C2 is exclusively monomeric, and Cy1-Cy2-A has a dissociation constant 2 orders of magnitude larger than those for multidomain subfragments containing C1. The contribution of Cy1-Cy2-A to the stabilization of the dimeric interface is not negligible. C1-PCP-C2 has a larger dissociation constant than Cy1-Cy2-A-C1 in a maximum likelihood sense (although the difference is not quite statistically significant ($P < 0.125$)), and this makes sense given that the dissociation constant for Cy1-Cy2-A is much lower than that for PCP-C2. It appears that Cy1-Cy2-A-C1 captures most of the binding free energy of full-length VibF, if one compares their respective dissociation constants: 118 ± 64 nM for Cy1-Cy2-A-C1 and 10−50 nM for VibF (*10*). Since C1 lies at the dimeric interface, the appropriate topological model for VibF places C1 at the core of the dimer, Cy1, Cy2, and A proximal to the interface, and PCP and C2 flanking at the sides of the complex. This model is supported by the weak but detectable self-association of Cy1-Cy2-A and by heterodimer mutant complementation experiments (*10*), which argue for placement of Cy1, Cy2, and A between PCP domains (because they are competent to operate on both intra- and interchain PCP domains on the time scale of the rate-limiting step) and C2 at the extremes (because it has a significant preference for the intrachain PCP domain on the time scale of the rate-limiting step). The best-fit monomer−dimer dissociation constant for the stand-alone C1 construct (176 ± 51 nM) is comparable to those for multidomain subfragments containing C1, and this shows that the C1 domain is self-sufficient to dimerize. This monomer−dimer dissociation constant should be considered an upper limit for C1, in that the performance of the dimer−tetramer model for C1 suggests that the monomeric state is not detectable with confidence at the experimental conditions. The formation of tetrameric C1 appears to occur at low micromolar concentrations of the subfragment. It is likely that this oligomeric state is not physiologically relevant to C1 function in the context of full-length VibF and may be an artifact of exposing the N- and C-termini of C1 to solvent, when under wild-type conditions it is flanked by the A and PCP domains.

Sedimentation equilibrium analytical ultracentrifugation experiments for the various VibF subfragment pairs provide estimates for the dissociation constants of the heterocomplexes between N- and C-terminal VibF subfragments. Reasonable heteroassociation model (A + B ↔ AB) data fitting indicates that Cy1-Cy2-A + PCP-C2 forms pseudo-VibF monomers (Cy1-Cy2-A·PCP-C2) but not pseudo-VibF dimers (Cy1-Cy2-A·PCP-C2)$_2$ to any significant extent. These results help resolve unanswered questions about the operation of wild-type VibF. While it has been shown that the functional oligomeric state of VibF is dimeric (*10*), it is not known whether the synthetase may additionally operate as a monomer. As a point of comparison, the related PKS and FAS systems function as dimers but not as monomers (*4*, *5*). Since Cy1-Cy2-A + PCP-C2 does not form pseudo-VibF dimers and this pair is competent to synthesize vibriobactin (*7*), it appears that a dimeric structure is not required for VibF function, in contrast with PKS and FAS synthases. It should be noted that this does not conclusively demonstrate that monomeric VibF is active, however, because covalent connectivity of Cy1-Cy2-A to PCP-C2 via C1 in wild-type VibF may place additional topological constraints between the domains that are not enforced in the disjointed subfragment pair. While previous studies investigated the linear rate of vibriobactin formation in the absence of the C1 domain for a given mixture of Cy1-Cy2-A + PCP-C2 (*7*), without the dissociation constant for Cy1-Cy2-A + PCP-C2 available, it was not previously possible to determine the turnover rate. With the dissociation constants for the pairs listed in Table 2, one may determine the k_{cat} values for the various heterocomplexes, listed in Table 3.

The turnover rates for the subfragment pair complexes vary from roughly 4- to 16-fold down from the established k_{cat} value for wild-type VibF of 48 min^{-1} (*10*). Cy1-Cy2-A·PCP-C2, (Cy1-Cy2-A-C1)$_2$·PCP-C2, and Cy1-Cy2-A·(C1-PCP-C2)$_2$ have statistically indistinguishable k_{cat} values and are all down 4-fold from Cy1-Cy2-A-C1·C1-PCP-C2. The equivalency of the three former complexes suggests that the mere presence of C1 adjacent to A or PCP does not appear to detectably enhance the catalytic rates of neighboring domains. On the other hand, Cy1-Cy2-A-C1·C1-PCP-C2 is the only complex with an intact C1 dimeric interface spanning the N- and C-terminal subfragments, and this could explain the differences in turnover rates, in that the C1 domains in Cy1-Cy2-A-C1·C1-PCP-C2 may properly orient Cy1-Cy2-A relative to PCP-C2. It is likely that the N- and C-terminal subfragments in the three former complexes do not entirely associate in the most productive conformation. To a certain extent, this suggests that monomeric VibF is active but not as active as the dimeric state, as the rank ordering of k_{cat} values (Cy1-Cy2-A·PCP-C2 < Cy1-Cy2-A-C1·C1-PCP-C2 < VibF) correlates with the extent to which each complex mimics dimeric VibF. The rate-limiting step in vibriobactin production is not known, but it is interesting to specifically note that (Cy1-Cy2-A-C1)$_2$·PCP-C2 and Cy1-Cy2-A·(C1-PCP-C2)$_2$ have statistically indistinguishable k_{cat} values, because the catalytic domain stoichiometries are reversed for the two complexes. If the rate-limiting step were largely due to Cy1, Cy2, or A, we would expect (Cy1-Cy2-A-C1)$_2$·PCP-C2 to be the faster of the two complexes. One explanation for the observation that neither subfragment pair mixture is faster is that there are two catalytic steps, one residing on each N- and C-terminal subfragment (e.g., those performed by Cy1 and C2), that are equally limiting. Another explanation would be that the protein dynamics required for catalysis in these artificial heterocomplexes are masking the rate-limiting step, because this would also result in indis-

tinguishable k_{cat} values.

The properties of the VibF C1 domain may be desirable for NRPS assembly line engineering. Removing C1 from VibF, generating the covalently contiguous construct Cy1-Cy2-A-PCP-C2, would likely result in a monomeric synthetase competent for the production of vibriobactin. In the converse experiment, inserting C1 into a related monomeric NRPS (e.g., the enterobactin synthetase EntF (C-A-PCP-TE) (*6*, *24*)) would yield (C-A-C1-PCP-TE) a novel, putatively dimeric form of the enzyme. Future studies will be needed to prepare the C1 deletion (Cy1-Cy2-A-PCP-C2 VibF) and insertion (C−A-C1-PCP-TE EntF) constructs to test these hypotheses. It should be noted that while the mere presence of C1 does not appear to affect the catalytic rates (and implicitly structural integrity) of neighboring domains, it remains unclear whether the imposed novel topologies of the C1 deletion and insertion constructs would yield active synthetases. Dimeric NRPS subunits may be of general utility to novel assembly line engineering for a number of reasons (beyond the catalytic domain orientation advantages specifically conferred to VibF). First, dimeric quaternary structure allows for alternate paths of intermediate elongation down the assembly line, in which the acyl-intermediates may jump from one NRPS protein chain to the other. A heterodimeric assembly line could thereby produce a combinatorial output, assuming substrate specificity tolerance of downstream domains. Second, dimeric synthetases with catalytic domains operating on both intra- and interchain tethered intermediates are expected to have longer functional lives because deleterious (e.g., oxidative) damage to a catalytic domain performing a non-rate-limiting step abrogates monomeric assembly line function but results in very little change to total product output in the case of dimeric complementation/redundancy (*10*). This operational life extension would be of interest for chemoenzymatic synthesis utilizing NRPS subunits, because enzymes would have to be replaced at a lower rate. Third, hybrid NRPS−PKS assembly lines are likely in general to be dimeric (*6*), and a dimeric exogenous NRPS subunit may be more compatible for insertion into a NRPS−PKS assembly line than its monomeric counterpart. Future studies will be required to test the versatility and utility of the VibF C1 domain as a general NRPS assembly line dimerization agent. An alternative strategy, if the structure of the C1 dimerization interface were known, would be to modify existing C domains in situ to mimic the relevant portions of C1.

ACKNOWLEDGMENT

We thank Susanne Swalley and the Harrison Lab for generously supplying ultracentrifugation time and Wei Lu and Frédéric Vaillancourt for reading of the manuscript.

REFERENCES

1. Smith, S. (1994) The animal fatty acid synthase: one gene, one polypeptide, seven enzymes, *FASEB J. 8*, 1248−1259.
2. Cane, D. E., and Walsh, C. T. (1999) The parallel and convergent universes of polyketide synthases and nonribosomal peptide synthetases, *Chem. Biol. 6*, R319−R325.
3. Marahiel, M. A., Stachelhaus, T., and Mootz, H. D. (1997) Modular Peptide Synthetases Involved in Nonribosomal Peptide Synthesis, *Chem. Rev. 97*, 2651−2673.
4. Staunton, J., Caffrey, P., Aparicio, J. F., Roberts, G. A., Bethell, S. S., and Leadlay, P. F. (1996) Evidence for a double-helical structure for modular polyketide synthases, *Nat. Struct. Biol. 3*, 188−192.
5. Joshi, A. K., Witkowski, A., and Smith, S. (1998) The malonyl/acetyltransferase and beta-ketoacyl synthase domains of the animal fatty acid synthase can cooperate with the acyl carrier protein domain of either subunit, *Biochemistry 37*, 2515−2523.
6. Sieber, S. A., Linne, U., Hillson, N. J., Roche, E., Walsh, C. T., and Marahiel, M. A. (2002) Evidence for a monomeric structure of nonribosomal peptide synthetases, *Chem. Biol. 9*, 997−1008.
7. Marshall, C. G., Hillson, N. J., and Walsh, C. T. (2002) Catalytic mapping of the vibriobactin biosynthetic enzyme VibF, *Biochemistry 41*, 244−250.
8. Keating, T. A., Marshall, C. G., and Walsh, C. T. (2000) Reconstitution and characterization of the *Vibrio cholerae* vibriobactin synthetase from VibB, VibE, VibF, and VibH, *Biochemistry 39*, 15522−15530.
9. Marshall, C. G., Burkart, M. D., Keating, T. A., and Walsh, C. T. (2001) Heterocycle formation in vibriobactin biosynthesis: alternative substrate utilization and identification of a condensed intermediate, *Biochemistry 40*, 10655−10663.
10. Hillson, N. J., and Walsh, C. T. (2003) Dimeric structure of the six-domain VibF subunit of vibriobactin synthetase: mutant domain activity regain and ultracentrifugation studies, *Biochemistry 42*, 766−775.
11. Henderson, D. P., and Payne, S. M. (1994) *Vibrio cholerae* iron transport systems: roles of heme and siderophore iron transport in virulence and identification of a gene associated with multiple iron transport systems, *Infect. Immun. 62*, 5120−5125.
12. Griffiths, G. L., Sigel, S. P., Payne, S. M., and Neilands, J. B. (1984) Vibriobactin, a siderophore from *Vibrio cholerae*, *J. Biol. Chem. 259*, 383−385.
13. Crosa, J. H., and Walsh, C. T. (2002) Genetics and assembly line enzymology of siderophore biosynthesis in bacteria, *Microbiol. Mol. Biol. Rev. 66*, 223−249.
14. Du, L., Sanchez, C., Chen, M., Edwards, D. J., and Shen, B. (2000) The biosynthetic gene cluster for the antitumor drug bleomycin from Streptomyces verticillus ATCC15003 supporting functional interactions between nonribosomal peptide synthetases and a polyketide synthase, *Chem. Biol. 7*, 623−642.
15. Tang, L., Yoon, Y. J., Choi, C. Y., and Hutchinson, C. R. (1998) Characterization of the enzymatic domains in the modular polyketide synthase involved in rifamycin B biosynthesis by *Amycolatopsis mediterranei*, *Gene 216*, 255−265.
16. Bevitt, D. J., Cortes, J., Haydock, S. F., and Leadlay, P. F. (1992) 6-Deoxyerythronolide-B synthase 2 from *Saccharopolyspora erythraea*. Cloning of the structural gene, sequence analysis and inferred domain structure of the multifunctional enzyme, *Eur. J. Biochem. 204*, 39−49.
17. Ikeda, H., Nonomiya, T., Usami, M., Ohta, T., and Omura, S. (1999) Organization of the biosynthetic gene cluster for the polyketide anthelmintic macrolide avermectin in *Streptomyces avermitilis*, *Proc. Natl. Acad. Sci. U.S.A. 96*, 9509−9514.
18. Schneider, T. L., Shen, B., and Walsh, C. T. (2003) Oxidase domains in epothilone and bleomycin biosynthesis: thiazoline to thiazole oxidation during chain elongation, *Biochemistry 42*, 9722−9730.
19. Patel, H. M., andd Walsh, C. T. (2001) In Vitro Reconstitution of the *Pseudomonas aeruginosa* Nonribosomal Peptide Synthesis of Pyochelin: Characterization of Backbone Tailoring Thiazoline Reductase and *N*-Methyltransferase Activities, *Biochemistry 40*, 9023−9031.
20. Sambrook, J., Fritsch, E. F., and Maniatis, T. (1989) *Molecular Cloning: A Laboratory Manual*, 2nd ed., Cold Spring Harbor Press, Plainview, NY.
21. UltraScan (6.0), http://www.ultrascan.uthscsa.edu. Accessed April 2004.
22. Laue, T. M., Shah, B. D., Ridgeway, T. M., and Pelletier, S. L. (1992) in *Analytical ultracentrifugation in biochemistry and polymer science* (Harding, S. E., Rowe, A. J., and Horton, J. C., Eds.) pp 90−125, Royal Society of Chemistry, Cambridge, U.K.
23. Cohn, E. J., and Edsall, J. T. (1943) *Proteins, Amino Acids and Peptides as Ions and Dipolar Ions*, Reinhold, New York.
24. Shaw-Reid, C. A., Kelleher, N. L., Losey, H. C., Gehring, A. M., Berg, C., and Walsh, C. T. (1999) Assembly line enzymology by multimodular nonribosomal peptide synthetases: the thioesterase domain of E. coli EntF catalyzes both elongation and cyclolactonization, *Chem. Biol. 6*, 385−400.

BI0489199